JOURNAL OF MATERIALS SCIENCE 32 (1997) 3869–3874

Characterization of molybdenum black coatings on zinc substrates

F. JAHAN*
Department of Applied Physics and Electronics, Rajshahi University, Rajshahi, Bangladesh

B. E. SMITH
Department of Mechanical Engineering, Brunel University, Uxbridge, Middlesex UB8 3PH, UK

Molybdenum black solar selective coatings have been prepared by a simple chemical conversion method on chemically etched zinc substrates. These coatings have been characterized using X-ray diffraction, electron diffraction, XPS and VIS-IR reflectance spectroscopy. Maximum solar absorptance obtained from these coatings was about 0.87 with an emittance of 0.13–0.17. Selectivity of the coatings, mainly attributed to the coating surface morphology, was studied by SEM. Structural studies show that the coating consists of a non-stoichiometric oxide of Mo, namely Mo_4O_{11}. XPS depth profiling studies show that the oxidation state of Mo reduces from $+5$ to $+4$ after argon ion bombardment.

1. Introduction

In our earlier communication [1] we have shown that the selectivity ($\alpha_s/\varepsilon_{th}$) of a Mo-black coating on a zinc substrate can be enhanced by substrate pretreatment. In this paper the deposition parameters, (such as temperature of the solution, deposition time) which yield the best radiative properties (α_s, ε_{th}) are described. Detailed characterization of the coatings studied by both scanning and transmission electron microscopy and X-ray photoelectron spectroscopy has been reported. The effect of heat treatment at different temperatures on the radiative properties of the coatings has also been described. Part of this work has been presented at the World Renewable Energy Congress [2].

2. Experimental details

2.1. Coating preparation

Commercially available zinc sheets of thickness 1 mm were used in the present work. To obtain uniform and adherent coatings, the thin surface oxide layer was removed from the zinc substrates by using emery paper of grades 600 and 1200 under a flow of water to avoid deep scratches. The substrates were then washed with distilled water, rinsed with alcohol and dried with compressed air. The second step was chemical etching. The zinc substrates were etched in 30% HNO_3 at a temperature of about 20 °C for a few seconds with constant stirring, followed by washing with distilled water, rinsing with alcohol and drying.

Following the pretreatment, zinc substrates were immersed in the plating solution. The plating solution consisted of ammonium paramolybdate $(NH_4)_6Mo_7O_{24}\cdot 4H_2O$ and nickel sulfate ($NiSO_4\cdot 6H_2O$). To obtain the optimum result (α_s, e_{th}) different concentrations of solution were used. The best results were obtained with 1 g $NiSO_4\cdot 6H_2O$ and 3 g $(NH_4)_6Mo_7O_{24}\cdot 4H_2O$ mixed in 150 cc of distilled water [3]. During deposition the solution was gently stirred in order to avoid non-uniformity and the formation of air bubbles. After deposition of the coatings they were washed with distilled water and dried with compressed air. The colour of the coating depended on the time of immersion and hence on the coating thickness. Until 20 s the coating was very thin and non-uniform. As the time of immersion increased the coating became darker and more uniform. The temperature of the solution influenced the coating thickness. Though the coating could be formed at low temperature, the rate of deposition was low. At high temperatures it was difficult to control the coating thickness due to the high deposition rate and the coating adhesion was poor. The best results were obtained in the temperature range 35–45 °C.

2.2. Characterization

The solar absorption (α_s) of the coatings were determined from reflectance measurements by using the method of selected ordinates [3, 4]. The total hemispherical reflectance (in the solar region 0.3 to 2.5 μm) of the coatings was measured by using a Beckman 5240 integrating sphere spectrophotometer. The thermal emittance (ε_{th}) was calculated from specular reflectance measurements in the infrared region (2.5 to 50 μm) using a Perkin Elmer (model 683) double beam ratio recording spectrophotometer with a reflectance attachment. A Cambridge Stereoscan 250 MK-2 scanning electron microscope (SEM) equipped with

* *Present address*: Department of Applied Physics, University of Technology, Sidney, Australia.

0022–2461

a solid-state detector was used to investigate the surface morphology of the coatings. Electron diffraction examination was performed by using a transmission electron microscope (model JEM7). The chemical composition of the coatings was analysed by X-ray photoelectron spectroscopy (XPS). The spectrometer (Kratos Analytical Instruments Ltd. Model ES300) employed monochromatized AlK_α radiation ($h\nu =$ 1486.6 eV) in a vacuum of $\sim 1.30 \times 10^{-5}$ Pa. The depth profile composition of the coatings was determined by using Ar^+ ion bombardment. The etching rate was roughly 0.1 nm min^{-1} with a 5 keV Ar^+ ion gun at a beam current of 5 mA. The atomic percentage of the chemical elements was determined by measuring the individual peak areas and dividing by their corresponding sensitivity factors [3].

3. Results and discussion

3.1. Spectral reflectance

The total reflectance spectra of Mo-black coatings on an etched zinc substrate are shown in Fig. 1 for different thicknesses (i.e. coating mass per unit area). No peaks are present in the region below 0.7 μm, except for the thinner coating where one peak appeared having a maximum at about 0.7 μm. The coatings have lowest reflectance in the UV and visible region. An interference minimum is present in the region 0.8 to 1.1 μm which is thought to be related to the band-gap of the coating materials [5]. This minimum hardly shifts towards the higher wavelength as the coating thickness increases. After this minimum, a transition takes place between high and low reflectance. In the near infrared (NIR) region, the reflectance decreases as the coating thickness increases and optical interference peaks are observed in the reflectance spectra.

The specular reflectance of the coating in the IR reflectance decreases with increasing coating mass resulting in an increase in emittance. The thinner coatings appear to be transparent to IR radiation, i.e. the thermal radiation is reflected from the substrate itself. As the coating thickness increases, the coating becomes opaque to IR radiation and the emittance increases. For the thickest coating, strong and broad absorption bands were observed in the region 10.5 to 22 μm (Fig. 2). The absorption peaks at about 6.2 μm and 2.9 to 3.1 μm indicate the presence of water in the coating [6].

The variation of α_s and ε_{th} with coating mass is shown in Fig. 3. The coating thickness was found to be critical for maximum solar absorption with a high selectivity factor. The absorption of the coating first increases sharply with coating thickness and attains a maximum value (0.87), while the increase in emittance is smaller. At this point the coating thickness was estimated to be in the range 0.15 to 0.25 μm. After that the emittance increases more rapidly with coating thickness and the absorption decreases slightly and then goes to the maximum value. Table I gives the values of α_s, ε_{th} and $\alpha_s/\varepsilon_{th}$ of the coating with coating mass.

The results indicate that a selectivity ratio $\alpha_s/\varepsilon_{th}$ of more than 6 can be obtained from these Mo-black

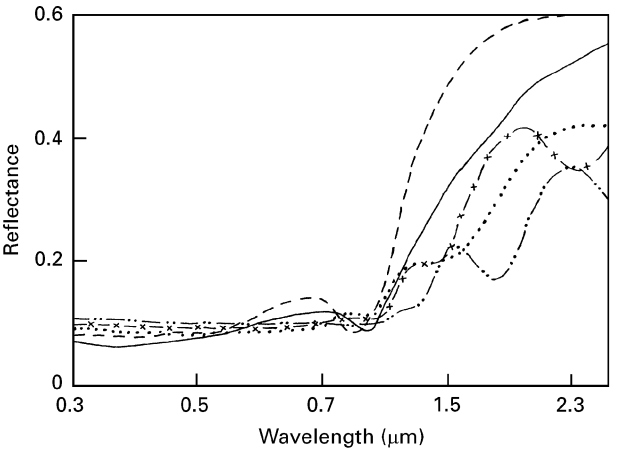

Figure 1 Spectral total reflectance of Mo-black coatings on zinc substrates for various coating mass per unit area, (– – – – – –) 0.039 mg cm^{-2}, (———) 0.065 mg cm^{-2}, (.....) 0.085 mg cm^{-2}, (×--×--×) 0.14 mg cm^{-2}, (–··–··–··–) 0.19 mg cm^{-2}.

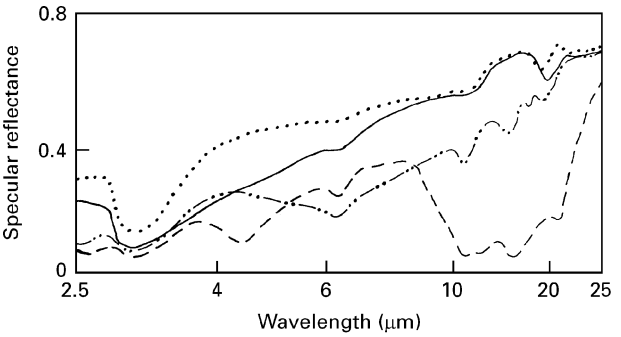

Figure 2 IR specular reflectance spectra of Mo-black dip coatings on zinc substrates for various coating mass per unit area, (.....) 0.039 mg cm^{-2}, (——) 0.065 mg cm^{-2}, (—··—··—) 0.102 mg cm^{-2}, (– – – –) 0.19 mg cm^{-2}.

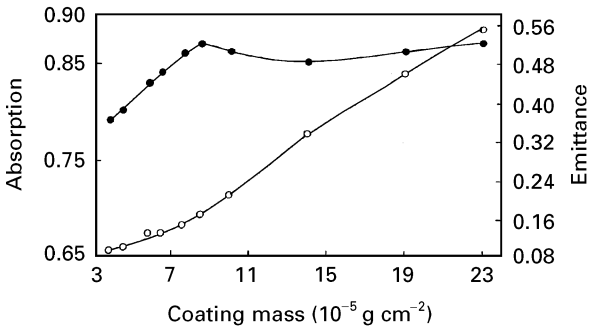

Figure 3 Variation of absorption α_s(●) and emittance ε_{th}(○) with coating mass per unit area of Mo-black dip coatings on zinc substrates.

TABLE I Absorption α_s, emittance ε_{th} and selectivity factor $\alpha_s/\varepsilon_{th}$ for Mo-black dip coatings on etched zinc substrate

Coating mass per unit area (mg cm^{-2})	α_s	ε_{th}	$\alpha_s/\varepsilon_{th}$
0.000	0.74	0.09	8.22
0.039	0.79	0.09	8.78
0.046	0.80	0.10	8.00
0.065	0.84	0.13	6.46
0.085	0.87	0.17	5.12
0.102	0.86	0.21	4.10
0.140	0.85	0.34	2.50
0.190	0.86	0.46	1.87
0.350	0.87	0.65	1.34

coatings on etched zinc substrates with a moderate absorption value (0.87). Agnihotri *et al.* [11] reported a selectivity ratio of 4.4 with $\alpha_s = 0.88$ for Mo-black coatings on galvanized steel sheets. In our earlier communication [1] it was shown that a high selectivity ratio ($\alpha_s/\varepsilon_{th} = 8.4$) was obtained from Mo-black coatings on mechanically polished zinc substrates with a rather low absorption value (0.76).

3.2. Structure and compositional analysis

Compositional and microstructural data are most important to the understanding of the physical processes responsible for selective absorption by a surface. The structure and composition of the Mo-black dip coatings were studied by scanning electron microscopy (SEM), X-ray photoelectron spectroscopy (XPS) and electron diffraction studies.

3.2.1. Electron diffraction studies

The reflection electron diffraction (RED) study of the coating indicates their polycrystalline nature (Fig. 4). The interplanar spacing values deduced from RED pattern gave evidence for the presence of Mo_4O_{11} in the coating. However some Mo_4O_{11} reflection lines are missing possibly due to buckling of the coating. As these dip coatings were too thin to be studied by X-ray diffraction, thick Mo-black coatings prepared by the electrodeposition method were studied by X-ray diffraction. A broad low angle peak corresponding approximately to the (2 0 0) interplanar spacing (1.23 nm) of Mo_4O_{11} was observed in the as-prepared coating. Study of a heat-treated coating (8 h in air at 400 °C) reveals the presence of a mixture of MoO_3 and Mo_4O_{11} in the coating. This suggests that the coatings are essentially crystalline though probably with some preferred orientation of (2 0 0) planes parallel to the substrate. The additional hypothesis of the presence of relatively small crystallites of Mo_4O_{11} and associated lattice defects together with high random microstrains is supported by transmission electron studies [3]. Potdar *et al.* [7] reported the presence of Mo_4O_{11} phase in the heat-treated (7 h at 390 °C) Mo-black coatings on nickel-plated copper substrates.

3.2.2. Micromorphology

A typical surface morphology of the optimum Mo-black coating on an etched zinc substrate is shown in Fig. 5a. The surface consists of a large number of nodules of different sizes ranging from 0.5 to 2 μm. The surface structure may reduce the front surface reflection and may also cause multiple reflections of the incoming solar radiation resulting in high solar absorption. It was reported earlier [1] that by using chemically etched zinc substrates rather than the mechanically polished ones, the absorption of Mo-black dip coatings increased by 14% and this is due to the difference in surface morphology. As the surface roughness is of the order of solar radiation wavelengths, it does not affect the emittance value significantly. By comparison of the topography of the etched zinc substrates with those of the coating, it seems that they are related, i.e. the coating is an outgrowth of the substrate itself. The coatings may start to grow as a large number of nodular structures

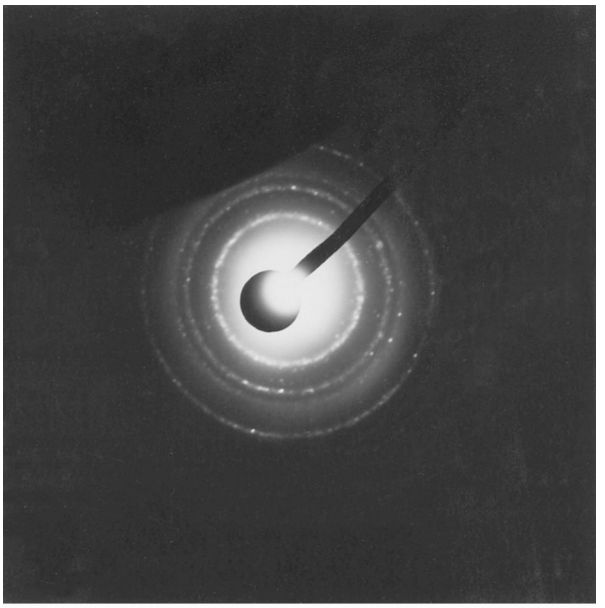

Figure 4 Reflection electron diffraction pattern of a Mo-black dip coating on a zinc substrate.

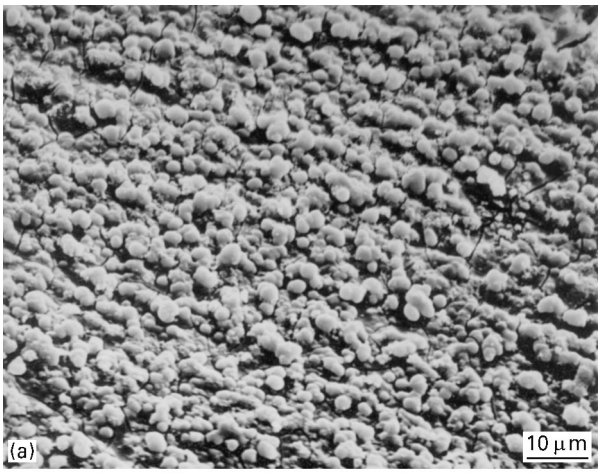

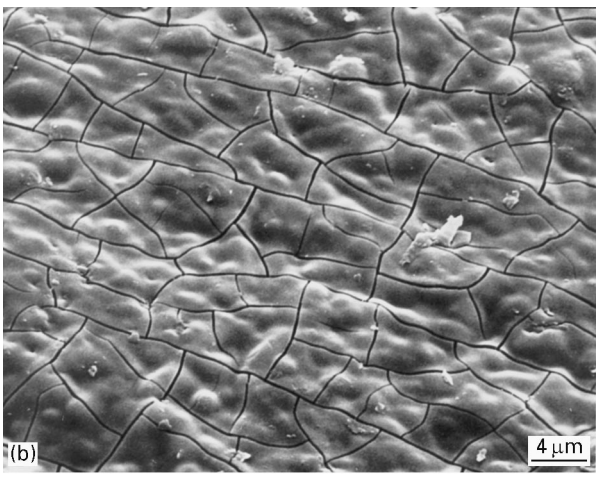

Figure 5 A typical SEM micrograph of a Mo-black coating on a zinc substrate: (a) optimum coating, and (b) thick coating.

on the substrate surface. As the coating thickness increases, the nodules gradually disappear and finally flat platelets with a wider cracked surface were observed as shown in Fig. 5b. This is probably due to the geometric levelling of the rough topography of the etched zinc.

As described in the previous section, the absorptance first increases sharply with coating thickness and then after attaining the maximum value it decreases slightly. The disappearance of the textured surface may be responsible for the slight decrease in absorption after the critical coating thickness. When the coating gets thicker then the absorption again increases slightly due to the thickness of the coating.

3.2.3. XPS studies

The elemental composition of Mo-black coating was analysed by XPS. The survey scan XPS spectrum (Fig. 6) of the coating shows that the coating consists of mainly molybdenum oxide and a small amount of nickel (the nickel peak is barely above the noise level). The appearance of C 1s peak originates from the spectrometer rotary pump oil that inevitably contaminates the samples at working pressure (1.3×10^{-5} Pa). In the present investigation, the chemical state of the constituent elements was determined by calculating the binding energy with reference to C 1s peak at 284.9 eV (which was found by calibration of the spectrometer). A different choice would change the actual value, not the relative value. For comparison, standard MoO_2, MoO_3 and Mo metal were also studied.

The survey scan spectra also shows O 1s, Auger and photoelectron peaks of zinc. The O 1s peak is at about 529.9 eV and is assigned to oxide oxygen [6]. The binding energy of Ni $2p_{3/2}$ peak was estimated to be 855.0 eV. The presence of strong broad satellite bands (Fig. 7) consistently at about 5.5 and 6.8 eV above the main peak of Ni $2p_{3/2}$ indicate the presence of $Ni(OH)_2$ in the coating. After etching with Ar^+ ions for 30 min, the satellite disappears but the binding energy of Ni $2p_{3/2}$ does not shift which is further evidence for the presence of $Ni(OH)_2$ in the coating [8].

The most intense peak of Mo is the Mo 3d doublet (Fig. 8). The first peak is at 231.4 eV and is assigned to Mo $3d_{5/2}$. The second peak is at 234 eV and is due to Mo $3d_{3/2}$. The binding energies (BE) of the Mo 3d doublet obtained from the Mo-black coating and the standard materials are given in Table II. This table clearly shows that the binding energies of Mo $3d_{3/2}$ and Mo $3d_{5/2}$ peaks for the Mo-black coatings are not consistent with that for $MoO_3(+6)$ nor $MoO_2(+4)$, but are in between $+6$ and $+4$. The basis of the chemical shift of a core photoelectron peak is the change in the electrostatic potential of the core electron when valence electron charge density is accepted or withdrawn from the atom [9]. There is, therefore, a relationship between the BE and the chemical state of the element. From our XPS analysis the oxidation state of Mo in the coatings is $+5$, which is close to that for Mo_4O_{11} as suggested from the RED study. In our work, the XPS study of Mo-black coating on other

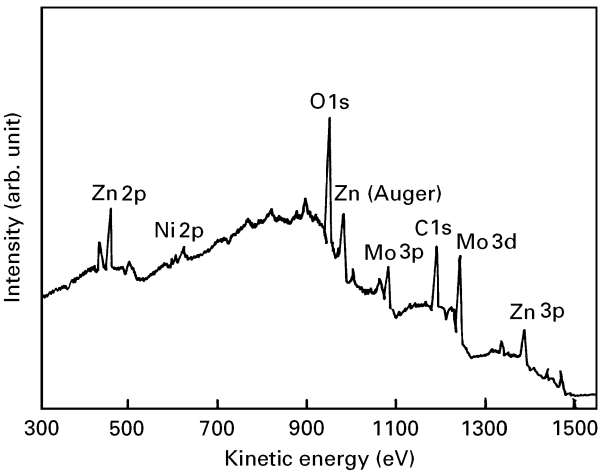

Figure 6 A survey scan XPS spectra of a Mo-black coating on a zinc substrate.

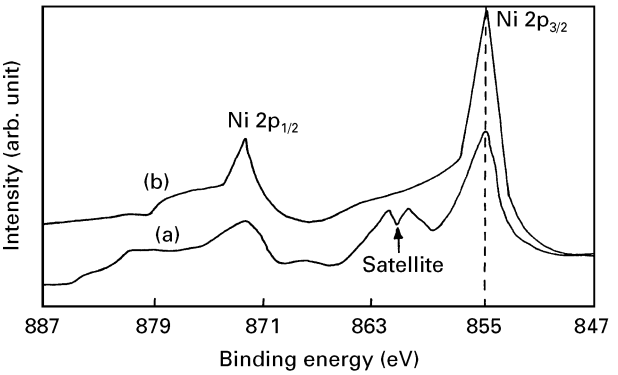

Figure 7 XPS spectra of nickel obtained from a Mo-black coating on a zinc substrate.

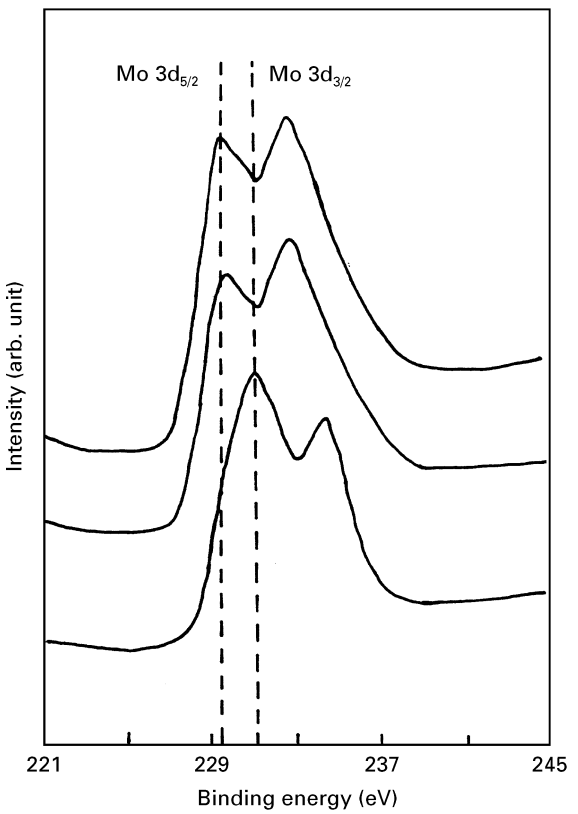

Figure 8 XPS doublet of Mo 3d obtained from a Mo-black coating on a zinc substrate: (a) as-prepared, (b) after 10 min etching, and (c) after 60 min etching.

TABLE II XPS data for Mo-black coatings on zinc substrates and standard material including shift in binding energy of Mo $3d_{5/2}$ peak with respect to that of Mo metal

Sample	Electron binding energy of Mo $3d_{3/2}$ (eV)	Electron binding energy of Mo $3d_{5/2}$ (eV)	Shift in binding energy (eV)	Oxidation state
Mo metal	230.2 + 0.2	227.0 + 0.1	0.0	0
MoO_2	232.4 + 0.2	229.3 + 0.2	2.3	+4
MoO_3	236.1 + 0.1	233.0 + 0.1	6.0	+6
Mo-black	234.0 + 0.1	231.4 + 0.2	4.4	+5

substrates (aluminium and electrodeposited cobalt on nickel-plated copper substrates) also shows similar results [3, 10]. Agnihotri *et al.* [11] reported the presence of MoO_3 in their Mo-black coating prepared from the same solution on galvanized steel sheet. According to their work the shift in BE of a Mo $3d_{5/2}$ electron of the Mo-black coating with respect to that for Mo metal is 2.8 eV. From our results (Table II) and also other published work [12] it can be seen that the shift in BE for MoO_3 is much higher than that obtained by Agnihotri *et al.* [11]. The shift in BE in their work indicates that the oxidation state of Mo in the coating is less than +6. Potdar *et al.* [7] described that the Mo-black coating on nickel-plated copper substrates consists of MoO_3. They have compared the BE of the Mo 3d doublet with the published value, which could be different due to the different reference value. However, they also reported that even at the surface of the coating, the ratio of O/Mo is less than expected for MoO_3. In the present work the ratio of O/Mo obtained from the coating is about 2.8 which is close to that for Mo_4O_{11}.

Mo-black coatings were also studied after heat treatment in air and vacuum. The coating oxidizes to +6 oxidation state (MoO_3) when heated in air at higher temperatures (390 °C). The dip coating reduces readily to the lower oxidation state (+4) when heated in vacuum. The shift in BE of the Mo $3d_{5/2}$ peak of the vacuum heated coating is 2.2 eV from the corresponding peak of Mo metal which is similar to the shift observed for MoO_2 (Table II). As zinc is a low melting point metal, heating of the coating may lead to diffusion of zinc through the coating. The coating might then be reduced to a lower oxidation state by zinc according to the following equation [13].

$$\text{Mo(V)oxide} + \text{Zn} = \text{Mo(IV)} + \text{ZnO}$$

Argon (Ar^+) ion bombardment was used to study the depth profile of the coating. After etching, the BE of the Mo 3d doublet is shifted towards that of MoO_2. Fig. 8 shows the Mo 3d spectra of the as-prepared coating and also at two different etching times. After 10 min etching with Ar^+ ions, the BE of the Mo $3d_{5/2}$ peak shifts from 231.4 to 229.9 eV. The peak shape also changed. The intensity of Mo $3d_{3/2}$ increased compared to the Mo $3d_{5/2}$ peak and also the Mo 3d doublet becomes broader. This indicates a mixture of two oxides, which are in a lower oxidation state than +6. These changes are thought to be due to the Ar^+ ion bombardment. The reduction of oxide to the lower oxidation state by Ar^+ ion etching is very common for most metal oxides. Some oxides even reduce to the metal [13]. However, in the case of Mo-black coatings no shift in BE beyond MoO_2(+4) was observed after Ar^+ ion bombardment over a prolonged time. It was also observed that the BE of the Mo 3d doublet of a vacuum heated coating, which is already in the +4 oxidation state (MoO_2 phase) does not shift after Ar^+ bombardment. These results are in agreement with the results reported by Kim *et al.* [14]. Potdar *et al.* [7] also reported reduction of Mo^{+6} to Mo^{+5} and Mo^{+4} species after Ar^+ ion etching of Mo-black coating on copper substrate.

The elemental composition of Mo-black coating was determined from XPS measurements. The atomic percentage of the chemical elements of the coating was calculated by measuring the individual main peak areas and dividing by their corresponding sensitivity factors. The atomic percentage of oxygen in the coating is about 72%, which is also consistent with the presence of Mo_4O_{11} in the coating. The atomic percentages of Mo, Zn and O_2 in a coating are shown in Fig. 9 as a function of etching time. The percentage of oxygen reduces to 57% in the first few minutes of etching, which may be due to the reduction of coating material to the lower oxidation state by the ion bombardment. It was also observed that the percentage of zinc decreases slightly over the first few minutes of etching and then remains the same until the substrate is exposed by thinning of the coating. The reason for the initial decrease of the zinc signal may be the healing up of the cracks by Ar^+ bombardment. Briggs and Seah [9] also reported that Ar^+ bombardment can induce changes in surface topography.

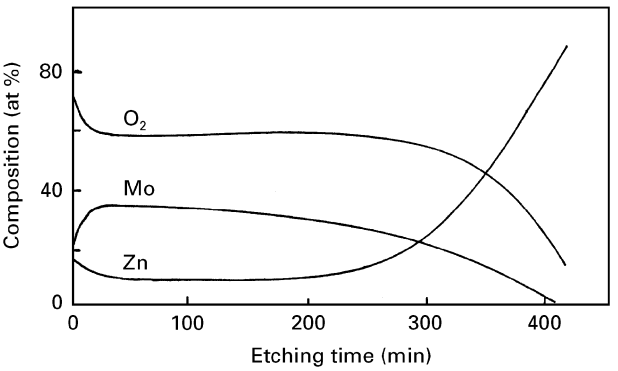

Figure 9 Composition depth profile of a Mo-black dip coating on a zinc substrate using Ar^+ ion bombardment.

3.3. Stability of Mo-black coatings

The thermal stability of these Mo-black coatings on etched zinc substrates was examined by heat treatment of the coatings in air and in vacuum of about 10^{-3} Pa at temperatures of 100, 150, 200 and 300 °C, for short period (4–24 h). The optimized coatings showed no degradation in these short-term heat-treatment tests. Fig. 10 shows the effect of heat treatment on the reflectance spectra of a coating at different temperatures. Small changes were observed in reflectance after heat treatment at temperatures of 100 and 200 °C. Heat treatment at 300 °C leads to dramatic changes in the reflectance spectra of the coating. The reflectance in the NIR region decreases substantially and this is accompanied by some increase of reflectance in the UV and visible region, resulting in no change in the solar absorption. It appears that the increase in the reflectance in the UV and visible region has been compensated for by the decrease in the NIR region. The emittance of the coatings also remain unchanged after heat treatment and in some cases decreases. The decrease in emittance is possible due to loss of water from the coatings. The infrared reflectance at longer wavelengths showed little change apart from loss of the water absorption band at 6.2 μm. The presence of nickel in the coating could also be responsible for the reduction of emittance. Decomposition of $Ni(OH)_2$ to NiO via dehydration and finally reduction in metallic Ni [15] could enhance the IR reflectance resulting in a decrease in emittance after annealing. Similar results were obtained when coatings were heat treated *in vacuo* but reflectance changes were generally smaller than those obtained after air heating. The durability of these coatings were also tested in natural conditions. A few coatings were left in outside ambient air facing southward (with shelter from direct rainfall, etc.) for five months. The values of α_s and ε_{th} remain effectively unchanged after such outdoor exposure.

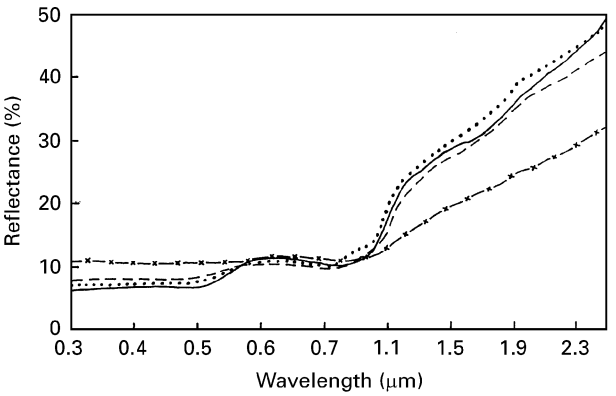

Figure 10 Effect of heat treatment on spectral reflectance spectra of a Mo-black coating on zinc substrate, (———) as-prepared, (.....) after heating at 100 °C for 8 h, (– – – –) after heating at 200 °C for 8 h, (-×--×-) after heating at 300 °C for 4 h.

References

1. F. JAHAN and B. E. SMITH, *J. Mater. Sci. Lett.* **5** (1986) 905.
2. F. JAHAN and B. E. SMITH, in Proceedings of the World Renewable Energy Congress, Reading, UK, 1990, published in "Energy of Environment", Vol. 3 (Pergamon Press, Oxford, 1990) p. 1368.
3. F. JAHAN, PhD thesis, Brunel University, UK (1987).
4. J. A. DUFFIE and W. A. BECKMAN, "Solar Engineering of Thermal processes" (John Wiley, New York, 1980) p. 146.
5. F. JAHAN, M. H. ISLAM and B. E. SMITH, *J. Solar Energy Mater. Solar Cells* **37** (1995) 283.
6. K. NAKAMOTO, "Infrared Spectra of Inorganic and Coordination Compounds" (Wiley-Interscience, New York, 1970).
7. H. S. POTDAR, A. B. MANDALE, S. D. SATHAYE and A. P. B. SINHA, *J. Mater. Sci.* **22** (1987) 2023.
8. T. ROBERT, M. BERTEL and G. OFFERGELD, *Surf. Sci.* **33** (1972) 123.
9. D. BRIGGS and M. P. SEAH, "Practical Surface Analysis by Auger and X-ray Photoelectron Spectroscopy" (John Wiley & Sons, New York, 1983).
10. F. JAHAN and B. E. SMITH, *J. Mater. Sci.* **27** (1992) 625.
11. G. P. AGNIHOTRI, B. K. GUPTA, A. K. AGARWAL and V. P. BHATNAGAR, *Thin Solid Films* **109** (1983) 193.
12. W. E. SWARTZ and D. M. HERCULES, *Anal. Chem.* **43** (1971) 1774.
13. J. A. VERCHERE and M. B. FLEURY, in Proceedings of the First International Conference on the Chemistry and Uses of Molybdenum, edited by P. C. H. Mitchel (Climax Molybdenum Co., London, 1975).
14. K. S. KIM, W. E. BAITINGER, J. W. AMY and N. WINOGRAD, *J. Electron. Spectrosc. Relat. Phenom.* **5** (1974) 351.
15. K. S. KIM and N. WINOGRAD, *Surf. Sci.* **43** (1974) 625.

Received 1 May 1995
and accepted 18 March 1996